Journal of Alloys and Compounds 495 (2010) 313–315

Contents lists available at ScienceDirect

Journal of Alloys and Compounds

journal homepage: www.elsevier.com/locate/jallcom

Evaluation of glass forming ability in the Ni–Nb–Zr alloy system by the topological instability (λ) criterion

F.S. Santos[a,*], C.S. Kiminami[b], C. Bolfarini[b], M.F. de Oliveira[c], W.J. Botta[b]

[a] Programa de Pós-graduação em Ciência e Engenharia de Materiais, Universidade Federal de São Carlos, Rodovia Washington Luiz, km 235, 13565-905 São Carlos, SP, Brazil
[b] Departamento de Engenharia de Materiais, Universidade Federal de São Carlos, Rodovia Washington Luiz, km 235, 13565-905 São Carlos, SP, Brazil
[c] SMM-EESC-USP, Av. Trabalhador São Carlense, 400, 13566-590 São Carlos, SP, Brazil

ARTICLE INFO

Article history:
Received 31 August 2008
Received in revised form 11 October 2009
Accepted 27 October 2009
Available online 6 November 2009

Keywords:
Metallic glasses
Rapid-solidification
Phase transitions
Thermal analysis
X-ray diffraction

ABSTRACT

Ni-based bulk metallic glasses (BMGs) usually exhibit high thermal stability, excellent mechanical properties, and superior corrosion resistance. Glass forming ability (GFA), which determines the critical amorphous size, limits the application of Ni-based BMGs. In the present work, we studied the ternary Ni–Nb–Zr alloy system, which shows relatively high GFA and the presence of passive-film-forming elements Nb and Zr that are beneficial for corrosion resistance. The GFA of the Ni–Nb–Zr alloy system was evaluated by the topological instability, λ criterion, used to calculate the minimum topological instability maps which indicate the compositions where the topological instability reaches the maximum among the surrounding stable phases. Such criterion was also combined with the electronegativity difference among the elements (Δe) in each particular composition, which it is assumed to be related to the formation enthalpy (ΔH) and glass stability of the corresponding alloy. The data from the literature for the maximum amorphous diameter were compared with the predictions of the topological λ criterion and with the combined criterion ($\lambda \times \Delta e$). Five compositions of rapidly solidified alloy ribbons were produced: $Ni_{45.5}Nb_{23}Zr_{31.5}$, $Ni_{50}Nb_{28}Zr_{22}$, $Ni_{57}Nb_{17.5}Zr_{25.5}$, $Ni_{62}Nb_{33}Zr_{5,}$ and $Ni_{79}Nb_{8.5}Zr_{12.5}$. Structures of the samples were examined by X-ray diffraction (XRD). Glass transition, crystallization and melting behavior were investigated by a differential scanning calorimeter (DSC). The combined criterion ($\lambda \times \Delta e$) provided specific guidelines for locating high glass-forming alloys in the Ni–Nb–Zr alloy system.

1. Introduction

Since the formation of the first metallic glass by rapid quenching reported by Klement et al. in 1960 [1], amorphous metals have attracted great scientific and technological interest. Ni-based bulk metallic glasses (BMGs) usually exhibit high thermal stability, excellent mechanical properties, such as high strength, hardness and good ductility, and excellent corrosion resistance [2,3]. The combination of these properties with low materials cost enables Ni-based BMGs to have promising applications as engineering materials, for example, pressure sensors and micro-geared motors [4,5]. However, the major drawbacks of Ni-based BMGs are the relatively low glass-forming ability (GFA) and small supercooled liquid region if compared with other BMGs, which limits their application.

The development of new amorphous alloys with high GFA has occurred through Inoue's empirical rules [6] and pinpointing. Recently, Kiminami et al. [7] proposed the lambda criterion (λ), a topological instability criterion for the selection of good glass-forming compositions. The minimum topological instability map background is the pioneer work of Egami and Waseda [8], which was later extended to predict the crystallization behavior of Al-rich amorphous alloys [9] and finally extrapolated for intermetallic phases in order to find the most favorable ranges of glass forming ability in binary Zr–Cu and ternary Zr–Cu–Al systems [7]. The later works are based on the named λ criterion, calculated from atomic radii or molar volumes of the compounds. The larger the λ parameter, the larger the topological instability of a crystalline solid solution. Assuming that a liquid is cooled fast enough to suppress long range diffusion as well as solute segregation, two choices are possible: crystallization of a solid solution (polymorphic) or amorphous formation. If a polymorphic transformation occurs, one would expect a solid solution with the smallest λ among the competing crystalline phases. Based on this assumption a minimum λ map is built in grayscale. The "peaks" on this map, depictured by brighter white points, express compositions where the topological instability reaches a maximum among the surrounding stable phases and thus a better glass forming ability is expected. Within a given system, the highest peaks are the most probable places

* Corresponding author. Tel.: +55 16 3351 8549.
E-mail addresses: fabricio_ssantos@yahoo.com.br (F.S. Santos), kiminami@ufscar.br (C.S. Kiminami), cbolfa@ufscar.br (C. Bolfarini), falcao@sc.usp.br (M.F. de Oliveira), wjbotta@ufscar.br (W.J. Botta).

0925-8388/$ – see front matter © 2009 Elsevier B.V. All rights reserved.
doi:10.1016/j.jallcom.2009.10.212

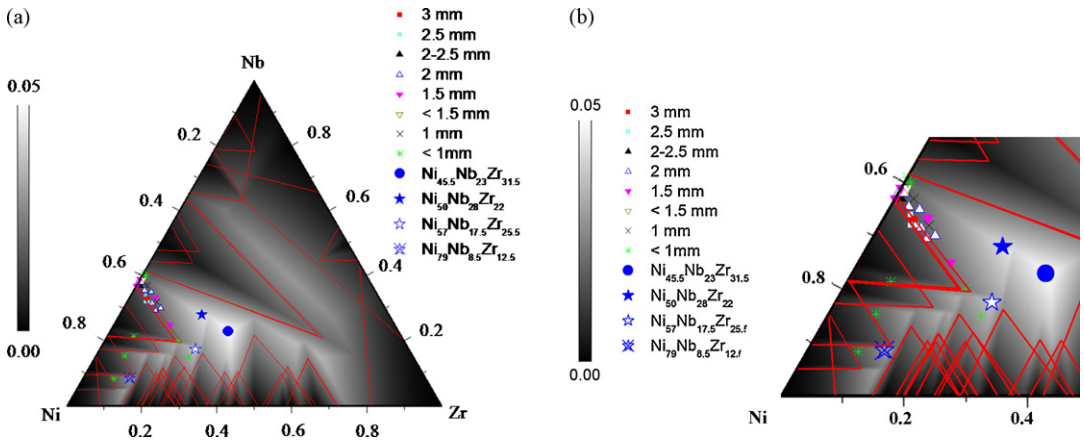

Fig. 1. Minimum λ and average electronegativity (λ × Δ*e*) map (in gray scale), λ = 0.1 lines (in red), and the amorphous critical diameter from the literature [13–16] for the Ni–Nb–Zr alloy system. (a) Ni–Nb–Zr composition triangle; (b) Ni-rich portion of the triangle. (For interpretation of the references to color in this figure legend, the reader is referred to the web version of the article.)

for good glass forming ability. The topological instability criterion, however, is not the only factor contributing for glass formation. In order to refine the λ minimum maps, another criterion is taken into account, the average electronegativity difference of one element and its surrounding neighbors in the alloy (Δ*e*). This parameter is calculated based on the assumption that the neighborhood around a central atom is dependent on the surface concentrations of atoms, used to weigh the electronegativity difference among each central atom and its neighbors. The overall average (Δ*e*) is weighted by the atomic fraction of each element [10]. The electronegativity difference among the elements of an alloy is directly related to its formation enthalpy (Δ*H*) and its glass stability [11,12]. Therefore, it is reasonable to suppose that the higher the average electronegativity difference among the elements, the higher the glass forming ability. Both factors are used together assuming a synergistic effect to produce a final criterion map resulting from simple multiplication of the topological instability and electronegativity criteria.

In this paper, we applied λ and Δ*e* criteria to investigate the GFA of the ternary Ni–Nb–Zr alloy system due to its relatively high GFA [13–16] and the presence of passive-film-forming elements Nb and Zr that are beneficial for corrosion resistance.

2. Experimental procedure

The GFA of the Ni–Nb–Zr alloy system was evaluated by the topological instability λ criterion [7], which was used to calculate minimum topological instability maps that indicate the compositions where the topological instability reaches the maximum among the surrounding stable phases. Such criterion was also combined with the electronegativity difference among the elements (Δ*e*) in each particular composition, which it is assumed to be related to the formation enthalpy (Δ*H*) and glass stability of the corresponding alloy [10]. The values of the combined criteria (λ × Δ*e*) in the composition triangle for the Ni–Nb–Zr system were used to search regions with higher peaks (depictured by brighter white points in the minimum λ × Δ*e* map). Alloy ingots with selected compositions were prepared by arc melting high-purity constituent elements, Ni (99.99%), Nb (99.8%), and Zr (99.5%) in a Ti-gettered high-purity argon atmosphere. The alloys were remelted under a high-purity argon atmosphere in a quartz tube and injected into a nozzle onto a Cu wheel to produce rapidly solidified ribbons by melt-spinning. Structures of the samples were examined by X-ray diffraction (XRD) with Cu Kα radiation. Glass transition, crystallization, and melting behavior were investigated by a differential scanning calorimeter (DSC) at the heating rate of 20 or 40 °C/min under a flowing Ar atmosphere, after preheating the samples (except the alloy composition $Ni_{62}Nb_{33}Zr_5$, produced for comparison purposes with the literature) below the crystallization temperature in order to promote structural relaxation and therefore evidence the glass transition behavior in the second heating.

3. Results and discussion

Fig. 1 shows the minimum λ × Δ*e* map, λ = 0.1 lines, and the amorphous critical diameter from the literature [13–16] for the system Ni–Nb–Zr. The λ = 0.1 lines represent the compositions for which the λ parameter is 0.1, that is the critical value for the topological instability of solid solution according to Egami and Waseda [8]. Considering a synergistic effect of topological and thermodynamic factors, the white regions in Fig. 1 represent compositions with high GFA. It can be seen that the alloys from the literature present critical diameters, up to 3 mm and are far from the white areas. Based on this map, the following four compositions were selected: $Ni_{45.5}Nb_{23}Zr_{31.5}$, situated at the brightest white point in the minimum λ × Δ*e* map, and $Ni_{50}Nb_{28}Zr_{22}$, $Ni_{57}Nb_{17.5}Zr_{25.5}$, and $Ni_{79}Nb_{8.5}Zr_{12.5}$, since these alloy compositions are situated in white areas in the map. For comparison purposes, the composition $Ni_{62}Nb_{33}Zr_5$ reported in the literature [13] was also selected.

Fig. 2 shows X-ray diffraction patterns of the melt-spun Ni–Nb–Zr alloys. The $Ni_{45.5}Nb_{23}Zr_{31.5}$, $Ni_{50}Nb_{28}Zr_{22}$, $Ni_{57}Nb_{17.5}Zr_{25.5}$, and $Ni_{62}Nb_{33}Zr_5$ ribbons present a diffused peak characteristic of amorphous structures. Furthermore, the $Ni_{57}Nb_{17.5}Zr_{25.5}$ alloy presents Bragg peaks of unknown crystalline phases. The $Ni_{79}Nb_{8.5}Zr_{12.5}$ ribbon shows Bragg peaks due to crystalline Ni, Nb, Ni_5Zr, and Ni_7Zr_2 phases. The full crystallinity of this ribbon was confirmed by thermal analysis, in which the DSC curve did not show any exothermic peak due to crystallization. Therefore, despite of the high values of λ × Δ*e* criterion, the cooling rate was not enough to produce a completely amorphous

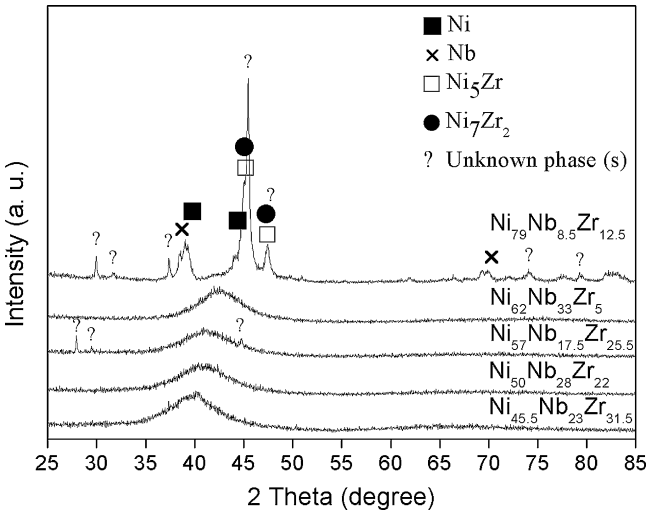

Fig. 2. X-ray diffraction (XRD) patterns of the melt-spun Ni–Nb–Zr alloys.

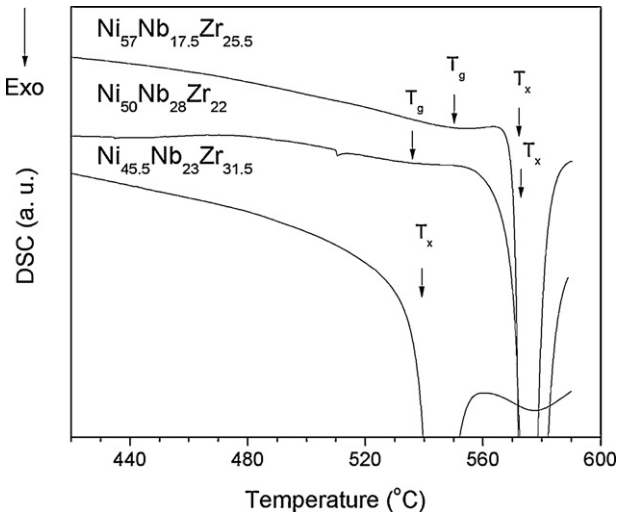

Fig. 3. DSC curves of the melt-spun Ni–Nb–Zr alloys.

Table 1
Glass transition (T_g), crystallization (T_x), solidus (T_s) and liquidus (T_l) temperatures, supercooled liquid region ($\Delta T_x = T_g - T_x$), and reduced glass transition temperature ($T_{rg} = T_g/T_l$) of the Ni–Nb–Zr alloys.

	T_g (°C)	T_x (°C)	T_s (°C)	T_l (°C)	ΔT_x (°C)	T_{rg}
$Ni_{62}Nb_{33}Zr_5$ [13]	604	644	1135	1212	40	0.591
$Ni_{62}Nb_{33}Zr_5$	605	647	1134	1203	42	0.590
$Ni_{45.5}Nb_{23}Zr_{31.5}$	–	539	1110	1228	–	–
$Ni_{50}Nb_{28}Zr_{22}$	536	573	1112	1133	37	0.575
$Ni_{57}Nb_{17.5}Zr_{25.5}$	550	572	1098	1147	22	0.580
$Ni_{79}Nb_{8.5}Zr_{12.5}$	–	–	1223	N/A	–	–

structure for $Ni_{79}Nb_{8.5}Zr_{12.5}$ and $Ni_{57}Nb_{17.5}Zr_{25.5}$ alloys produced by melt-spinning. Considering that melt-spinning provides nearly the same solidification cooling rate, since the alloys studied in this work have similar physical properties such as thermal conductivity, the rapid solidification process by melt-spinning reveal that the $Ni_{45.5}Nb_{23}Zr_{31.5}$, $Ni_{50}Nb_{28}Zr_{22}$ and $Ni_{62}Nb_{33}Zr_5$ alloys show the better glass forming ability, followed by the $Ni_{57}Nb_{17.5}Zr_{25.5}$ and $Ni_{79}Nb_{8.5}Zr_{12.5}$ alloys (in that order).

Fig. 3 shows DSC curves of the melt-spun Ni–Nb–Zr alloys. The $Ni_{50}Nb_{28}Zr_{22}$ and $Ni_{57}Nb_{17.5}Zr_{25.5}$ alloys exhibit an endothermic event characteristic of glass transition, whereas the $Ni_{45.5}Nb_{23}Zr_{31.5}$ alloy does not manifest glass transition. Thermal data analysis of the thermograms: glass transition (T_g), crystallization (T_x), solidus (T_s) and liquidus (T_l) temperatures, supercooled liquid region ($\Delta T_x = T_g - T_x$), and reduced glass transition temperature ($T_{rg} = T_g/T_l$) are listed in Table 1. The thermal data for the $Ni_{62}Nb_{33}Zr_5$ alloy are in agreement with those from the literature [13] giving validity for the processing procedures used in the present experiment.

Correlations between glass forming ability and thermal data such as ΔT_x and T_{rg} have been reported in the literature [6]. Although these correlations are not general, i.e., they are not always valid for all the alloys, they have commonly been used for evaluate the glass forming ability of alloys, since the critical cooling rate is difficult to be measured experimentally. For the new compositions investigated in this work, although not presenting T_g, the $Ni_{45.5}Nb_{23}Zr_{31.5}$ alloy ribbon was fully amorphous (confirmed by XRD, Fig. 2), as forecasted due to its high topological instability indicated by the high value of $\lambda \times \Delta e$ parameter. The high T_{rg} values of the $Ni_{50}Nb_{28}Zr_{22}$ and $Ni_{57}Nb_{17.5}Zr_{25.5}$ alloys (0.575 and 0.580 respectively) give an indication of high GFA [6]. These alloys are located in the white areas in $\lambda \times \Delta e$ map (Fig. 1). Particularly, for the $Ni_{50}Nb_{28}Zr_{22}$ alloy, a single melting peak on the heating and small temperature range between T_s and T_l (21 °C) indicates that this composition is close to the eutectic point explaining its high GFA that can be correlated with its high T_{rg} and the fully amorphous structure confirmed by the XRD (Fig. 2). The $Ni_{79}Nb_{8.5}Zr_{12.5}$ ribbon was completely crystalline, which can be ascribed to its high Ni content and its position, which is close to the regions of topological stability of several phases as showed by the red lines in Fig. 1.

4. Conclusions

The use of both λ and Δe criteria was successfully applied to investigate the GFA of the Ni–Nb–Zr alloy system and select good glass-forming compositions. From the four compositions proposed, three ($Ni_{45.5}Nb_{23}Zr_{31.5}$, $Ni_{50}Nb_{28}Zr_{22}$, $Ni_{57}Nb_{17.5}Zr_{25.5}$) showed amorphous structures when processed by melt-spinning, and the thermal crystallization data analysis shows agreement with this behavior.

Acknowledgements

The authors are grateful for the financial support provided by FAPESP (The State of São Paulo Research Foundation), "Projeto Temático" no. 2005/59594-0 and scholarship no. 06/60964-0.

References

[1] W. Klement, R.H. Willens, P. Duwez, Nature 187 (1960) 869–870.
[2] T. Zhang, A. Inoue, Mater. Trans. 43 (2002) 708–711.
[3] S.J. Pang, C.H. Shek, K. Asami, A. Inoue, T. Zhang, J. Alloys Compd. 434 (2007) 240–243.
[4] N. Nishiyama, K. Amiya, A. Inoue, J. Non-Cryst. Solids 353 (2007) 3615–3621.
[5] M. Ishida, H. Takeda, N. Nishiyama, K. Kita, Y. Shimizu, Y. Saotome, A. Inoue, Mater. Sci. Eng. A 449–451 (2007) 149–154.
[6] A. Inoue, Acta Mater. 48 (2000) 279–306.
[7] C.S. Kiminami, R.D. Sá Lisboa, M.F. de Oliveira, C. Bolfarini, W.J. Botta, Mater. Trans. 48 (2007) 1739–1742.
[8] T. Egami, Y. Waseda, J. Non-Cryst. Solids 64 (1984) 113–134.
[9] R.D. Sá Lisboa, C. Bolfarini, W.J. Botta, C.S. Kiminami, Appl. Phys. Lett. 86 (2005) 211904.
[10] W.J. Botta, F.S. Pereira, C. Bolfarini, C.S. Kiminami, M.F. de Oliveira, Phil. Mag. Lett. 88 (2008) 785–791.
[11] S.S. Fang, Z.Q. Zhou, J.L. Zhang, M. Yao, F. Feng, D.O. Northwood, J. Alloys Compd. 293–295 (1999) 10–13.
[12] S.S. Fang, X.S. Xiao, L. Xia, W.H. Li, Y. Dong, J. Non-Cryst. Solids 321 (2003) 120–125.
[13] L.Y. Chen, H.T. Hu, G.Q. Zhang, J.Z. Jiang, J. Alloys Compd. 443 (2007) 109–113.
[14] H.J. Chang, E.S. Park, Y.S. Jung, M.K. Kim, D.H. Kim, J. Alloys Compd. 434 (2007) 156–159.
[15] Z.W. Zhu, H.F. Zhang, W.S. Sun, Z.Q. Hu, J. Mater. Res. 22 (2007) 453–459.
[16] A.P. Wang, J.Q. Wang, J. Mater. Res. 22 (2007) 1–4.